Antarctic Science 21 (3), 301–312 (2009) © Antarctic Science Ltd 2009 Printed in the UK doi:10.1017/S0954102009001825

Representation of the Weddell Sea deep water masses in the ocean component of the NCAR-CCSM model

RODRIGO KERR[1]*, ILANA WAINER[2] and MAURICIO M. MATA[1]

[1]*Laboratório de Estudos dos Oceanos e Clima, Instituto de Oceanografia, Universidade Federal do Rio Grande (FURG), Rio Grande, RS, 96201-900, Brazil*

[2]*Laboratório de Meteorologia Marinha, Dept. de Oceanografia Física, Instituto Oceanográfico, Universidade de São Paulo, São Paulo, SP, 05508-120, Brazil*

**pgofkerr@furg.br*

Abstract: We examine Weddell Sea deep water mass distributions with respect to the results from three different model runs using the oceanic component of the National Center for Atmospheric Research Community Climate System Model (NCAR-CCSM). One run is inter-annually forced by corrected NCAR/NCEP fluxes, while the other two are forced with the annual cycle obtained from the same climatology. One of the latter runs includes an interactive sea-ice model. Optimum Multiparameter analysis is applied to separate the deep water masses in the Greenwich Meridian section (into the Weddell Sea only) to measure the degree of realism obtained in the simulations. First, we describe the distribution of the simulated deep water masses using observed water type indices. Since the observed indices do not provide an acceptable representation of the Weddell Sea deep water masses as expected, they are specifically adjusted for each simulation. Differences among the water masses' representations in the three simulations are quantified through their root-mean-square differences. Results point out the need for better representation (and inclusion) of ice-related processes in order to improve the oceanic characteristics and variability of dense Southern Ocean water masses in the outputs of the NCAR-CCSM model, and probably in other ocean and climate models.

Received 16 April 2008, accepted 12 December 2008

Key words: Antarctic, Greenwich Meridian, modelling, OMP analysis, Southern Ocean

Introduction

The study of oceans and the atmosphere using complex coupled climate models has acquired significant importance in explaining climate variability and climate change as well as the role of the oceans in atmospheric variability. Although much attention is paid to understanding interface variables, such as the sea surface temperature (SST), sea level pressure, and surface winds, not much is known about the behaviour of the hydrographical properties of the deep ocean in these complex models. The dense water masses acquire their signatures directly from air-sea processes, which makes them excellent indicators of climate change.

The Southern Ocean has an important role in both local and global climate as a result of the complex interactions between ocean, atmosphere, and sea-ice, which impact the global thermohaline circulation. In this context, the Weddell Sea (Fig. 1) is a very important region because of its dominant role in the production and export of Antarctic Bottom Water (AABW) to the world ocean (e.g. Carmack 1977, Orsi *et al.* 1999).

The water column in the Weddell Sea can be divided into three main layers: i) the surface, i.e. top 200 m of water column, ii) intermediate, between 200 and 1500 m, and iii) deep, below 1500 m. This pattern is also found in the region of the Weddell Gyre, which includes the entire Weddell–Enderby Basin (Fig. 1). Small changes in depth may occur depending on the area of the gyre being considered. The water mass characteristics of these three layers are as follows.

Surface water masses are near freezing and are seasonally influenced. The atmospheric and sea-ice conditions are the main factors that control the temperature and salinity of these waters. Smaller scale ice processes that involve production rates and durations of coastal polynyas are also important in defining Shelf Water characteristics. These are yet to be resolved by higher resolution models and are not considered in this study. In Southern Ocean coastal regions, newly ventilated Shelf Waters differ mainly by their salinity values. High Salinity Shelf Water (HSSW) and Ice Shelf Water (ISW), with salinity ranges between 34.56–34.84 and 34.2–34.7, respectively (Robertson *et al.* 2002), are the main Shelf Waters that contribute to dense water mass formation in the south-western Weddell Sea (Foster & Carmack 1976, Foldvik *et al.* 1985). Away from the shelves, in the oceanic regime, a layer of winter water (i.e. a remnant of the deep winter mixed layer) exists below the surface waters throughout the summer.

The intermediate and deep layers consist of Warm Deep Water (WDW), Weddell Sea Deep Water (WSDW), and

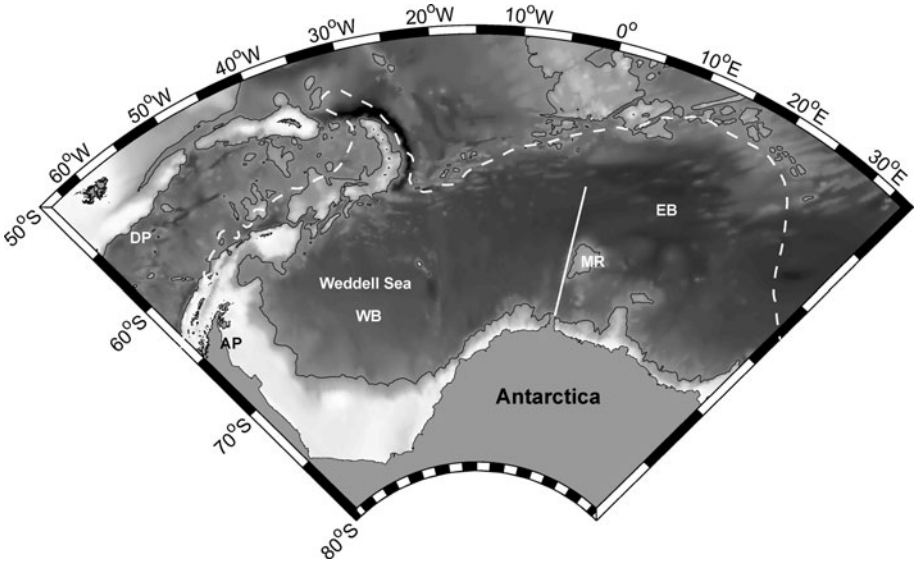

Fig. 1. Study area and its bathymetry (black line shows 3000 m isobath). Thicker white line represents the Greenwich Meridian longitude-depth section analysed in this study. Southern boundary of the Antarctic Circumpolar Current is shown by dashed white line (same as Orsi *et al.* 1995). AP = Antarctic Peninsula, DP = Drake Passage, EB = Enderby Basin, WB = Weddell Basin, and MR = Maud Rise.

Weddell Sea Bottom Water (WSBW). The WDW is another main water mass contributing to the formation of deep waters in the Weddell Sea. It originates from the Circumpolar Deep Water (CDW) within the Antarctic Circumpolar Current (ACC) and joins the gyre circulation between 20°E and 30°E (Gouretski & Danilov 1993). As CDW is advected into the Weddell Gyre, its temperature and salinity characteristics change due to mixing with Surface and Shelf Waters, resulting in WDW, which is cooler and fresher than the original CDW. In fact, Gordon & Huber (1984) show that the temperature maximum of the WDW is mostly below 0.5°C during the end of winter stratification near 60°S between 5°E and the Greenwich meridian, but also note that warmer cells of WDW, with potential temperature-salinity (θ/S) values similar to the WDW characteristic of the inflow area, can be found in some regions of the Weddell Gyre. Foster & Carmack (1977) consider Modified Warm Deep Water (MWDW), a mixing product between WDW and the winter water layer, as a transitional water mass present in the Weddell Sea.

WSDW results from mixing between WDW and/or MWDW with WSBW, and is formed by deep convection mainly along the shelf break in the south-western Weddell Sea, but also may form directly depending on the source water properties (Orsi *et al.* 1993, Weppernig *et al.* 1996). The WSDW becomes AABW as it escapes from the Weddell Sea, while WSBW is topographically constrained and remains within the Weddell Basin. The WSBW outflow only occurs through mixing with the WSDW above or through a few deep passages (see Fahrbach *et al.* 1995, Orsi *et al.* 1999). It should be noted that the distinction between WSDW and WSBW is based on different source water types with WSBW resulting from the mixing of WDW or MWDW with either ISW (Foldvik *et al.* 1985) or HSSW (Carmack & Foster 1975).

Several observational studies have described the vertical distribution of hydrographical parameters in the Weddell Sea (e.g. Carmack & Foster 1975, Deacon 1979, Fahrbach *et al.* 1994, 2001, Gordon 1998, Gordon *et al.* 2001). However, these studies are limited by temporal and spatial data coverage. To overcome this limitation, numerical models have become excellent tools. However, considering the inherent difficulties in dealing with the deep ocean, model results need to be extensively assessed and validated in the Southern Ocean.

This study aims to compare deep water mass distribution (below 500 m depth) in different simulations conducted with the ocean component of the National Center for Atmospheric Research Community Climate System Model (NCAR-CCSM). We also compare model results with World Ocean Circulation Experiment (WOCE) data. We have a particular interest in how the inclusion of an interactive sea-ice model affects the representation of deep ocean characteristics in the NCAR-CCSM model.

Simulations and NCAR-CCSM model configurations

Three model runs using different forcing fields and configurations have been analysed in the Greenwich Meridian section in the Weddell Sea (Fig. 1). This section was chosen because several hydrographical transects have been carried out in the region (e.g. Fahrbach *et al.* 2004, Klatt *et al.* 2005), which allows for a direct comparison between observations and model results. The first experiment (hereafter referred to as POP-INT) consists of the ocean component of the NCAR-CCSM forced by 43 years of Large & Yeager (2004) fluxes. The second and third experiments (hereafter referred to as POP-NOICE and POP-CORE1, respectively) are forced by a repeat annual cycle obtained from the Large & Yeager (2004) forcing developed for coupled ocean-ice models. The POP-CORE1

https://doi.org/10.1017/S0954102009001825 Published online by Cambridge University Press

Table I. Analysed Model Outputs.

Model	Acronyms	Type (resolution)	Forced with
Parallel Ocean Program (POP3)	POP-INT	Ocean-only ($1^\circ \times 1^\circ$)	Interannual forcing using NCEP/NCAR winds forcing with corrected fluxes over ice-covered regions, 43 yr (Large & Yeager 2004)
	POP-NOICE	Ocean-only ($1^\circ \times 1^\circ$)	Annual cycle using NCEP/NCAR winds and fluxes
	POP-CORE1	Ocean model ($1^\circ \times 1^\circ$) coupled to an interactive sea-ice model (CSIM)	Annual cycle using NCEP/NCAR winds and fluxes

simulation is the same run used in the Coordinated Ocean Ice Reference Experiments (COREs), discussed in Griffies *et al.* (2009). It consists of the ocean component of the NCAR-CCSM coupled to the Community Sea-ice Model (CSIM, Briegleb *et al.* 2004). The CSIM serves as the sea-ice component of CCSM. It is the result of a community effort to develop a portable, efficient sea-ice model that can be run coupled to a global climate model or uncoupled as a stand-alone ice model. It is a dynamic-thermodynamic model that includes a sub-grid scale ice thickness distribution, energy conserving thermodynamics, and elastic viscous plastic (EVP) dynamics. POP-NOICE is not coupled to the CSIM. The runs are summarized in Table I.

The ocean component of the NCAR-CCSM solves the primitive equations in general orthogonal coordinates in the horizontal with the hydrostatic and Boussinesq approximations. Although this study focuses on the Weddell Sea, the model domain is global. The grid uses spherical coordinates in the Southern Hemisphere, but in the Northern Hemisphere the pole is displaced into Greenland at 80°N, 40°W. The horizontal grid has 320 zonal and 384 meridional grid points, and the resolution is uniform zonally but not meridionally. In the Southern Hemisphere, the meridional resolution is 0.27° at the equator, gradually increasing to 0.54° south of 33°S, and is constant at higher latitudes. There are 40 levels in the vertical, whose thickness increases monotonically from 10 m near the surface to 250 m in the deep ocean. The minimum depth is 30 m, and the maximum depth is 5.5 km. The surface fresh water flux is converted into an implied salt flux using constant reference salinity. Therefore, although the sea surface height varies locally, the ocean volume remains fixed. The time step used is one hour. The horizontal viscosity is a Laplacian operator that is anisotropic following the formulation of Smith & McWilliams (2003), and uses different coefficients in the east–west and north–south directions. Both coefficients vary in space and time, depending on the local rates of shear and strain, and the minimum background horizontal viscosity is 1000 $m^2 s^{-1}$. The vertical mixing scheme is the KPP scheme of Large *et al.* (1994). Further details on the ocean component of the CCSM3 can be found in Smith & Gent (2004).

The model forcing follows Large & Yeager (2004) and is also described in Griffies *et al.* (2009). The interannual forcing is composed of a 40 yr cycle (1958–1997) of 6-hourly winds near surface temperature and humidity from the National Center for Environmental Prediction (NCEP)–NCAR reanalysis. The model starts from a resting state of observed temperature and salinity distributions and is integrated until the solution has lost all memory of the initial conditions (the spin-up is 500 years). The model is then run for four 43 yr forcing cycles. The analysis is restricted to the fourth cycle. The repeat annual cycle (Normal Year Forcing, NYF) consists of a normal year constructed to retain synoptic variability (i.e. Yeager & Large 2007). A detailed description of the NCAR-CCSM model configuration and biases can be found in the June 2006 special issue of the *Journal of Climate.*

Optimum Multiparameter Analysis (OMP)

We have chosen to use the Optimum Multiparameter (OMP) technique to trace Weddell Sea deep water masses in this study. This method was introduced by Tomczak (1981) as an extension of classical water mass analysis through temperature-salinity (T/S) diagrams (Mamayev 1975). Mackas *et al.* (1987) and Tomczak & Large (1989) significantly improved the multiparameter analysis, showing the potential of the method to analyse mixing conditions and water mass distribution in both coastal and oceanic regions.

Some definitions are needed to fully understand the physical basis of the multiparameter analysis (Tomczak & Large 1989). First, a water mass is defined as a physical entity that occupies a finite volume in space (Tomczak & Large 1989) or as a body of water with a common formation history with its source in specific parts of the ocean (Tomczak 1999). Second, the water masses are defined by water types, which refer to a set of hydrographical parameters that describe the properties of the water masses, or by source water types, which are a set of hydrographical parameters that describe the properties of newly formed water masses (Tomczak & Godfrey 1994).

The OMP analysis quantifies mixing between selected water masses (i.e. water type percentage contribution to the total mixture) by solving an over-determined system of linear mixing equations that use several conservative and semi-conservative parameters. In matrix form, this can be written as:

$$Gx = d + r \tag{1}$$

https://doi.org/10.1017/S0954102009001825 Published online by Cambridge University Press

Table II. Water types, parameters and weights used for OMP input.

Water mass	Parameter simulation depth (m)	Potential temperature (°C)				Salinity			
		POP-INT	POP-NOICE	POP-CORE1	NODC	POP-INT	POP-NOICE	POP-CORE1	NODC
WDW	500–1000	0.8	0.5	0.8	0.5	34.667	34.662	34.685	34.70
WSDW	1500–4000	-0.1	-0.3	-0.1	-0.3	34.667	34.666	34.660	34.66
WSBW	> 4000	-0.9	-0.9	-0.6	-0.9	34.659	34.656	34.650	34.64
Parameter weight		7.2	5.8	8.6	11.5	0.2	0.1	1.1	11.5

where G is the matrix of water types, x is the OMP result (i.e. fractions of each water type), d is the vector of observed data (or model outputs as addressed in this study), and r is the vector of residuals. The mixing equations are normalized to make parameters with different units comparable, and the equations are weighted to account for environmental variability and/or measurement uncertainty (see below). This system of equations (Eq. 1) is solved by minimizing the residuals (r) in a least squares sense, which yields the optimum combination of water type contributions.

The standard OMP analysis package (OMP2 2005) is used here to estimate the distribution and fractions of mixture of the Weddell Sea deep water masses (based on local water mass definitions - i.e. water types) in the NCAR-CCSM simulations described above. The limited number of available hydrographical parameters restricts the number of water masses used to run the OMP. From the model simulations considered here, only potential temperature (θ) and salinity are considered, which means that the number of water types that can be used to separate the water masses with OMP is limited to three. Thus, the following water masses are considered in this study: WDW, WSDW, and WSBW. Only two physical restrictions are imposed in the OMP analysis: the first is mass conservation, which means that the contribution of all water types must add up to 100%, and second, this contribution cannot be negative.

It is necessary to gauge the system of mixing equations to account for environmental variability and/or measurement accuracy. Weights are obtained from parameters variance (see Tomczak & Large 1989 for more details). Input parameters with higher weights will have greater influence than parameters of lower weights to construct the final water mass distribution. In this study, high applied weights are correlated with parameters that are further realistic represented in the ocean simulations. Resolving the contribution of the deep water mass or those water masses which have only a very small gradient within the parameters used is directly associated with the established weights. Therefore, it is necessary to restrict the analysis to a depth range where homogeneous weights may be applied (J. Karstensen, personal communication 2007), e.g. disregarding the variable and well-mixed surface layer and considering only deep waters for the OMP application (this study). Although it is relatively easy to trace the mixing of only three water masses through the T/S diagram, applying the OMP technique leads to refined results (M. Tomczak, personal communication 2006). A detailed description, advantages, and other applications of the OMP method can be obtained from Tomczak & Large (1989), Karstensen & Tomczak (1997, 1998), and Leffanue & Tomczak (2004).

The OMP technique is applied to the model outputs in two different approaches. The first considers water type indices from historical observed data, while the second uses indices calculated from model climatology (Table II). The observed water types used in the first approach are calculated using *in situ* data obtained from the National Oceanographic Data Center (NODC) historical hydrographical dataset. In this case, the weights (Table II) were obtained using the variance equation described in Tomczak & Large (1989). For the second OMP application, the water type indices were adjusted to better represent model water masses, for which θ and salinity may differ somewhat from observed water masses characteristics. This was accomplished using modelled θ and salinity values found in selected depth intervals (see Table II). In this case, the parameter weights were calculated based on the variances of the water types and of the model θ/S outputs.

Weddell deep ocean representation in the NCAR-CCSM model

The ocean component of the NCAR-CCSM model has been extensively studied and validated against observations (e.g. Large *et al.* 1997, Gent *et al.* 1998, Danabasoglu 2004, Large & Danabasoglu 2006). According to these studies, observations and model results are in good agreement with respect to gyres and inter-basin exchanges, despite the generally too strong near-surface winds. Drake Passage (Fig. 1) transport is too strong but has little effect on SST and sea surface salinity. Doney & Hecht (2002) note that the surface boundary conditions in permanent sea-ice covered regions are leading to inadequate formation of dense, cold, and relatively saline shelf waters, which is an important precursor of the dense source water masses that form AABW. The origins of the Southern Ocean water masses have been the subject of much investigation but their rates of formation and contributions to global ocean ventilation are still under debate.

https://doi.org/10.1017/S0954102009001825 Published online by Cambridge University Press

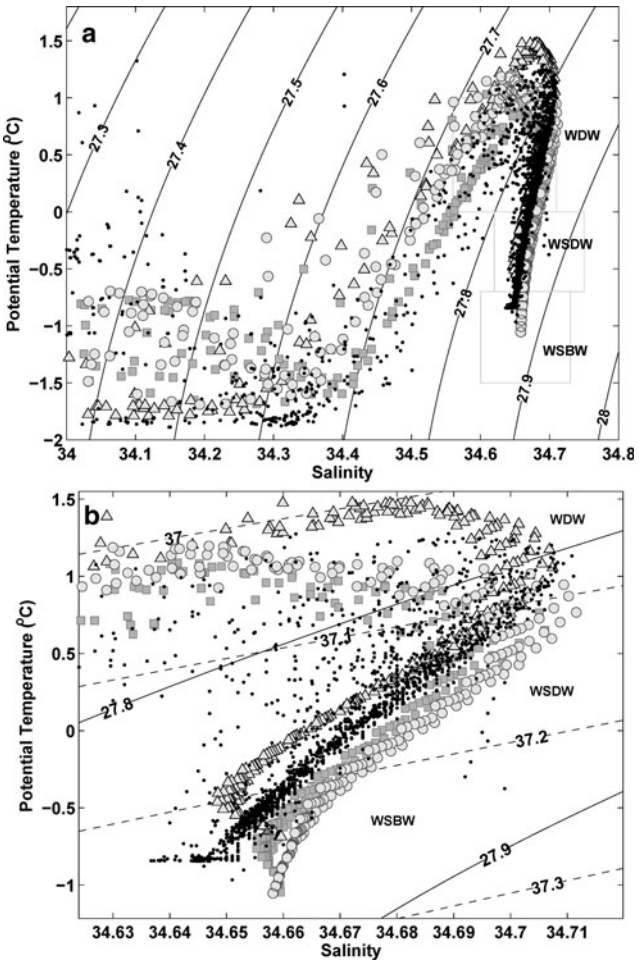

Fig. 2. a. Full range potential temperature-salinity diagram for POP-INT (circles), POP-NOICE (squares) and POP-CORE1 (triangles) simulations and the NODC/NOAA dataset (dots) at the Greenwich Meridian for the years 1984, 1986, 1992, 1996, and 1998, which were used to obtain the observed mean water mass distribution in Fig. 7. The rectangles limit water masses based on Robertson *et al.* (2002). **b.** Same as (a) but zoomed in on the salinity of deep water masses. Solid lines indicate σ_0 and dashed lines σ_2.

Some of the densest water masses in the Southern Ocean are dependent on salinity/freshwater fluxes from the marine cryosphere (i.e. sea-ice, icebergs, and ice shelves). Thus, the inclusion of sea-ice related processes, as well as coupling a sea-ice model to general global circulation models is a desirable model development goal (e.g. Fichefet & Maqueda 1997, Lipscomb & Hunke 2004, Holland *et al.* 2006, Huntley *et al.* 2007). Climate models do not normally represent the fluxes from icebergs and ice shelves. Recently, advances in parameterizing ice shelf processes and representing the flow within ice shelf cavities have been discussed and included in both regional and global models (e.g. Timmermann *et al.* 2002, Beckmann & Goosse 2003, Thoma *et al.* 2006). For example, Thoma *et al.* (2006) showed that changes in ice shelf configurations have significant impacts on the water mass properties of the eastern Weddell Sea.

The integration period for the simulations present here may be shorter than the equilibrium time for the middle to deep oceans. However, this work focuses at model-model intercomparison so the integration time is sufficient to reveal differences between models and drift with respect to observations. Examinations of the integrated mean kinetic energy (KE), and the KE per layer for each of the simulations (not shown) reveal that the runs are dynamically stable. With respect to temperature and salinity, there is a fast initial adjustment with small drifts in the deeper oceans, but it should be noted that the present analysis relies on mean properties, not variability or changes in the thermohaline properties of the Southern Ocean.

As can be seen in the θ/S diagram for the Greenwich Meridian region (Fig. 2), neither simulation exactly represents the observed absolute θ/S values for the entire water column. Ocean only simulations (i.e. POP-INT and POP-NOICE runs) represent the WDW layer more realistically than do simulations with the interactive sea-ice model (i.e. POP-CORE1 run). The latter show the highest temperature values for the WDW layer. The layer that encloses the WSDW and WSBW is badly represented in all simulations. In general, while for POP-INT and POP-NOICE these waters are saltier and colder, including the interactive sea-ice model renders the WSDW and WSBW fresher and warmer. Biases with respect to the CORE-I simulation results are discussed in Griffies *et al.* (2009), where the most notable are found exactly in the Southern Ocean, suggesting the importance of examining ice-ocean interactions and feedbacks. The sections of θ and salinity and their differences with respect to observations can be seen in Figs 3 & 4.

The θ section of each simulation (Fig. 3a–c) clearly shows the WDW core in the intermediate layer up to 1500 m despite small differences in the absolute values of θ. However, significant differences exist in the deep ocean representations. Both the POP-INT and POP-NOICE simulation results are colder (~0.3°C) than those with the interactive sea-ice model. The θ-difference (Fig. 3d–f) shows the simulated WDW layer (i.e. 500–1500 m) with temperature cores in excess of 0.5, 0.3, and 0.5°C warmer for the POP-INT, POP-NOICE, and POP-CORE1 runs, respectively. Considering the layer between 1500 and 2000 m, which is the mixing zone between WDW and WSDW, the simulated temperature is still warmer with respect to observations. For this depth interval, the ocean-only runs shows that θ varies between 0.1 and 0.4°C for POP-INT (Fig. 3a), and -0.1 and 0.2°C for POP-NOICE (Fig. 3b), which is 0.2 to 0.5°C higher than the observed values for this layer (Fig. 3d & e). POP-CORE1 simulations show a pattern similar to that described for

https://doi.org/10.1017/S0954102009001825 Published online by Cambridge University Press

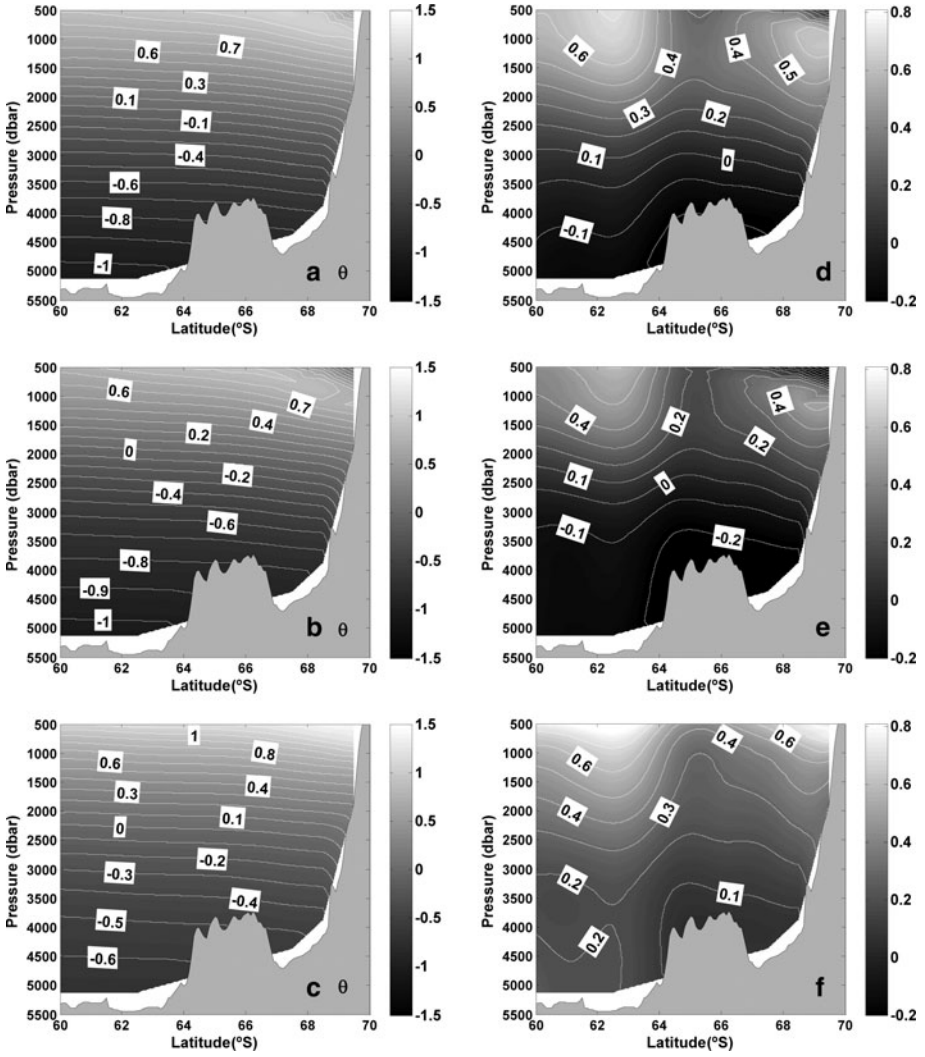

Fig. 3. a–c. Potential temperature (θ) distribution, and **d–f.** θ-difference (simulated minus observation) for POP-INT, POP-NOICE, and POP-CORE1 simulations, respectively, in the Greenwich Meridian section for depths >500 m.

POP-INT. Between 2000 and 4000 m (i.e. the WSDW layer), distinct patterns are evident for each simulation. For POP-INT (Fig. 3d), this layer displays temperatures approximately 0.1 to 0.3°C warmer than the observations for the upper levels, while POP-NOICE simulations show temperatures in general 0.1 to 0.2°C lower (Fig. 3e). On the other hand, for the POP-CORE1 results, the WSDW layer is approximately 0.2°C warmer (Fig. 3f). Below 4000 m, the ocean-only runs yield temperatures 0.1 to 0.2°C colder (Fig. 3d & e) than POP-CORE1 (Fig. 3f).

The POP-CORE1 run simulates salinity better for the Greenwich section (Fig. 4c) than the ocean-only runs (Fig. 4a & b). The WDW core with salinity 34.7 is displaced upward and salinities around 34.65 appear near the bottom, better characterizing this region (Fig. 4c), but there are still differences. The highest reported salinity difference (i.e. 0.015 to 0.03 saltier; Fig. 4d–f) up to 1500 m shows that the WDW layer is saltier for all simulations than the observed data. Conversely, the deep ocean (between 2000 and 4000 m) shows salinity values slightly saltier than the observations, but without differentiating the WSDW and WSBW layers for the POP-INT and POP-NOICE simulations (Fig. 4d & e). The POP-CORE1 simulation produces a relatively fresh core around 3000 m (Fig. 4f), with salinity values near observed values, which may indicate the first step to better representing the WSBW layer. The salinity values that differentiate the water masses considered in this study are very similar, making it difficult to characterize the water masses in the water column. Further discussion of this matter is presented in the next sections.

Representation of the Weddell Sea Deep Water masses from observations

The mean water mass distribution from observations obtained by Kerr (2006) is shown in Fig. 5. This mean distribution was obtained from the OMP analysis for each repeat section sampled on the Greenwich line, which considered in the years 1984, 1986, 1992, 1996, and 1998

https://doi.org/10.1017/S0954102009001825 Published online by Cambridge University Press

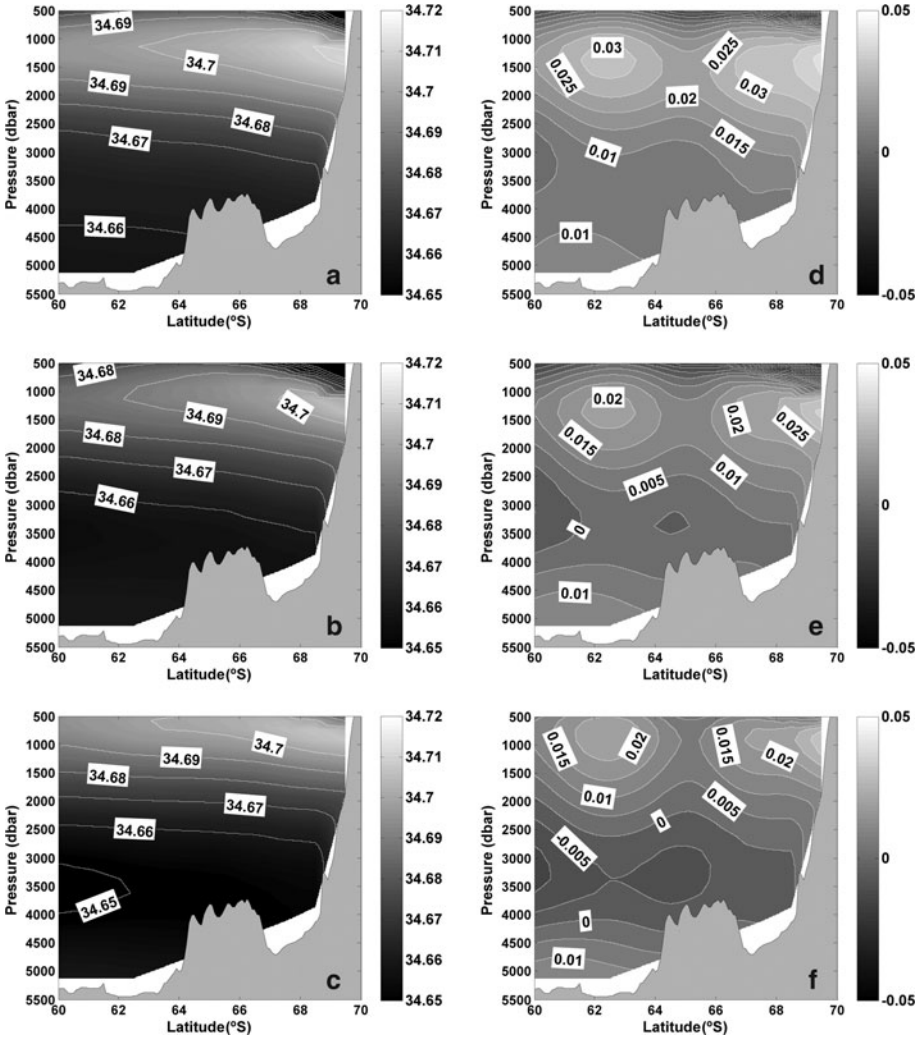

Fig. 4. Same as Fig. 3, but for salinity field.

(for more details see Kerr 2006). Klatt *et al.* (2005) and Fahrbach *et al.* (2004) describe the characteristic properties and the variability of this area. The water mass structure of the Greenwich Meridian section is well captured, showing the WDW occurring in the intermediate layer down to ~2000 m representing more than 30% of the contribution to the water column (Fig. 5a). The WSDW core contribution is above 50%. It is distinct between 1000–3500 m (Fig. 5b), and the WSBW is present below 3000 m (> 50%) with a greater contribution (> 70%) below 4000 m in the region north of the Maud Rise (Fig. 5c).

Representation of the Weddell Sea Deep Water masses in the NCAR-CCSM

There is a growing need to investigate the performance of the Southern Ocean water mass properties in ocean general circulation models (OGCMs). Recently, Connolley &

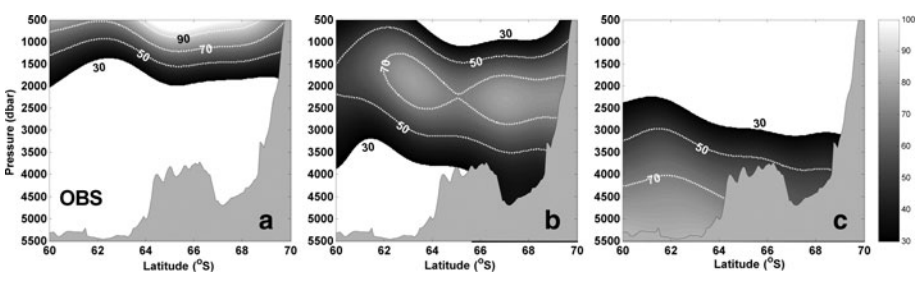

Fig. 5. Observed (OBS) mean water mass distribution (% of mixing) from the NODC/NOAA dataset at the Greenwich Meridian for the years 1984, 1986, 1992, 1996, and 1998, using the water types based on NODC data (see Table II). **a.** Warm Deep Water, **b.** Weddell Sea Deep Water, and **c.** Weddell Sea Bottom Water. The seamount is the Maud Rise.

https://doi.org/10.1017/S0954102009001825 Published online by Cambridge University Press

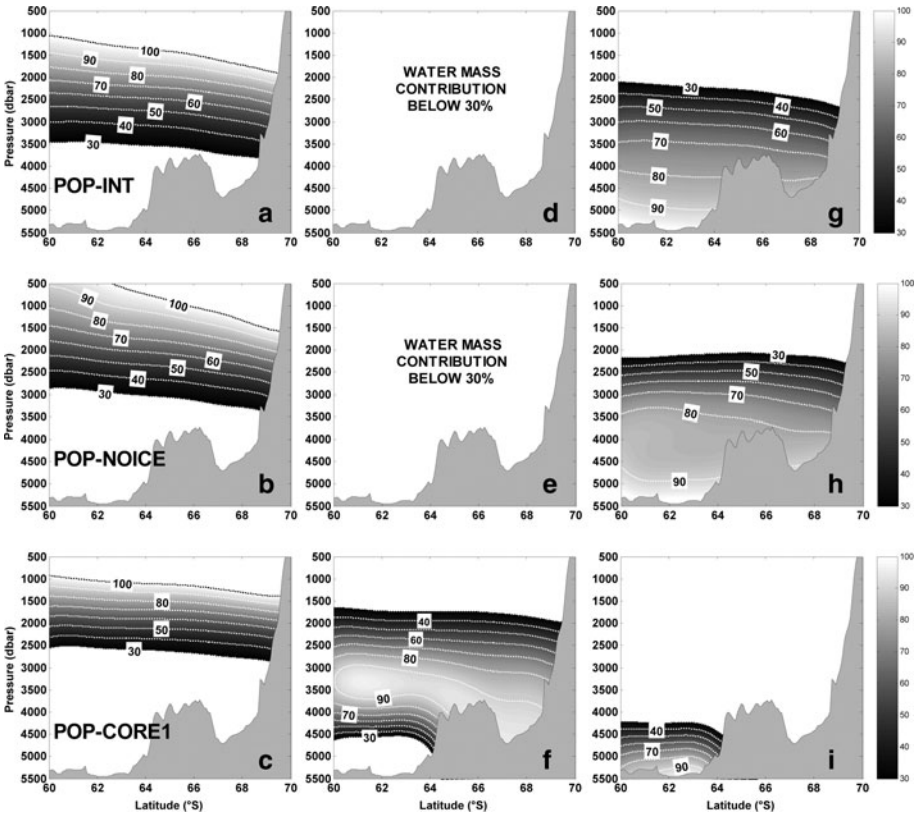

Fig. 6. Dense water mass distribution (% of mixing) at the Greenwich Meridian section obtained from POP-INT, POP-NOICE, and POP-CORE1 simulations, as indicated in the first box, using the water type index based on NODC data (see Table II). Each column indicates specifics water masses: **a–c.** Warm Deep Water, **d–f.** Weddell Sea Deep Water, and **g–i.** Weddell Sea Bottom Water. The seamount is the Maud Rise.

Bracegirdle (2007) carried out an Antarctic assessment of several IPCC AR4 coupled models and showed that the NCAR-CCSM did not score high when compared with other models. In fact, climate models in general do a poor job of representing water masses, in particular with respect to the Southern Ocean. One reason may be that climate models do not accurately represent the ice-ocean interactions necessary for proper water mass formation, ventilation, and spreading. The lack of vertical resolution could also be a problem in correctly representing the Antarctic water masses.

The present study addresses this issue by performing an OMP analysis on Weddell Deep Water Masses represented in the ocean component of the NCAR-CCSM model. It should be noted that the concept of the water type used to fingerprint water masses is an artificial quantitative analysis construction that does not occupy any volume in space (Tomczak & Large 1989). The OMP analysis simply allocates the water mass that is closer in parameter space to the water type definition used regarding the hydrographical properties.

Two approaches are considered when using the OMP analysis with the NCAR-CCSM model outputs. First, water types are obtained from observed data (i.e. calculated from the NODC historical dataset). Next, taking into account the overall differences between model-simulated and observed water mass characteristics, the OMP technique is applied using redefined water types. The redefined water types are adjusted for each specific simulation. This approach embraces more precisely the deep water masses in each different run. The root-mean-square (RMS) differences between the water mass representations obtained from model results and NODC data are calculated to assess the OMP outputs.

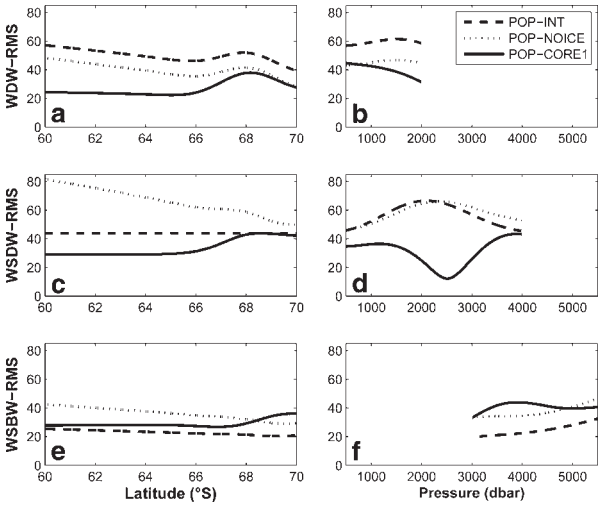

Fig. 7. Root-mean-square difference (RMS) for dense water masses analysed with observed water types in the Greenwich Meridian section. **a, b.** Warm Deep Water (WDW), **c, d.** Weddell Sea Deep Water (WSDW), and **e, f.** Weddell Sea Bottom Water (WSBW). For all graphics, each simulation is represented as indicated in (b).

https://doi.org/10.1017/S0954102009001825 Published online by Cambridge University Press

Water mass representation with observed water types

OMP results obtained from the model simulations show that the ocean-only runs (i.e. POP-INT and POP-NOICE) do not adequately represent the water mass distribution in the Weddell Sea (Fig. 6). The layer thickness of WDW and WSBW is overestimated in both simulations. As can be seen in the POP-INT simulation results (Fig. 6a), the WDW contribution reaches high values in the mixture (between 50–70%) at levels below 2000 m, which is an unrealistic depth for this water mass (see Fig. 5a). The same is true for the WDW in the POP-NOICE simulation results (Fig. 6b); i.e. a high water mass contribution (between 50–70%) at deeper levels. Using observed water type indices yields an unrealistic WDW distribution and incorrect mixture fractions at the intermediate water column for both ocean-only runs.

As both WDW and WSBW are overestimated in the POP-INT and POP-NOICE runs, it is not surprising that the OMP analysis yields an unrealistic distribution for the WSDW (Fig. 6d & e). In these two simulations, the WSDW contribution to the total mixture was below 30% (Fig. 6d & e). Tracing WSDW in the water column becomes difficult because of the occurrence of this water mass throughout a wide depth range (i.e. approximately 3000 m) and a relatively large temperature range (for example, between 0 and -0.7°C for the WSDW). These facts may indicate that more than one water type should be used to mark that particular water mass in the ocean as suggested in the OMP technical report for some specific cases (OMP2 2005). However, the unrealistic separation of the Weddell Sea water masses presented here is probably associated with: i) the choice of the water type salinity index (Table II), considering the closer salinity range in the deep layers of the Weddell Sea (Fig. 4), and ii) the use of equal weights applied for θ and salinity in this approach, which does not account for the fact that the temperature field is better represented than the salinity field (with respect to the observations). WSBW is also overestimated in POP-INT and POP-NOICE (Fig. 6g & h). The expected outcome would be WSBW predominant ($>$ 70%) below 4000 m, but in the simulation WSBW is displaced upwards. The OMP results show contributions $>$ 70% below 3500 m (Fig. 6g) and below 3000 m (Fig. 6h) for POP-INT and POP-NOICE, respectively.

The POP-CORE1 simulation yields a somewhat more realistic water mass distribution than other runs when compared with observations (e.g. Fahrbach *et al.* 2004, Kerr *et al.* 2005), as illustrated by the smallest RMS difference (Fig. 7). This is a significant result that indicates the importance of including a sea-ice model to improve regional representation of dense water masses in ocean models. The improvement is probably due to the fact that the simulated salinity values are closer to the observed. WDW occurs down to a depth of 2000 m with contributions above 50% in the model (Fig. 6c). The WSDW occupies the layer between 2000–4200 m with contributions higher than 50% (Fig. 6f), and the WSBW is confined to the deep oceanic basin north of Maud Rise (Fig. 6i). However, differences still occur when the simulated water mass distribution is qualitatively compared to the observed (Fig. 5).

In summary, the interactive sea-ice model yields an overall vertical displacement of the simulated deep water masses relative to observations. Changes related to the contribution of each water mass are also noted. This reflects the lack of coastal processes representation in the model (such as coastal polynyas and local sea-ice formation). These govern the formation of Shelf Waters in the model configuration, which could lead to inaccurate deep water mass properties. As reported by Large & Danabasoglu (2006), near-surface regions has not been well captured by simulations using the ocean component of the NCAR-CCSM model, and small systematic displacements will lead to large SST biases due to strong horizontal gradients.

We calculate RMS differences in order to quantify disparities among water mass representations. The greatest agreement between the numerical representations of WDW, WSDW, and WSBW is for the smallest implied normalized RMS differences (or observational uncertainty) between the OMP results. The run in which the sea-ice model is interactive has the smallest RMS (Fig. 7). The salinity results from POP-INT are not sensitive enough to allow separation between the WSDW and WSBW (they yield one water mass only) in this OMP analysis, which explains why its associated RMS difference with respect to the observations is less for the WSBW (Fig. 7e & f).

Salinity has a fundamental role in determining the density field in the polar regions. Thus, any salinity change will significantly impact water mass distribution. NCAR-CCSM ocean simulations do not reproduce the observed salinity patterns exactly, as demonstrated by the salinity differences shown in Fig. 4d–f. Salinity patterns are better simulated in the POP-CORE1 run, suggesting that it is necessary to couple with a sea-ice model to correctly simulate deep salinity values, and consequently, deep water mass characteristics. As it stands, salinity corrections are needed to identify specific deep water masses. However, this is not the ultimate solution for correctly representing the dense water mass characteristics (see discussion below). Including other cryospheric processes in the model is also necessary, as are improvements in the sea-ice parameterizations.

Water mass representation using water types adjusted to each individual simulation

Here, the θ/S structure for each experiment is examined separately (see Fig. 2). Water types and weights used to perform the OMP analysis are adjusted for each analysed simulation (see Table II). Unlike the previous results, an observation-based water type index is used for each water

https://doi.org/10.1017/S0954102009001825 Published online by Cambridge University Press

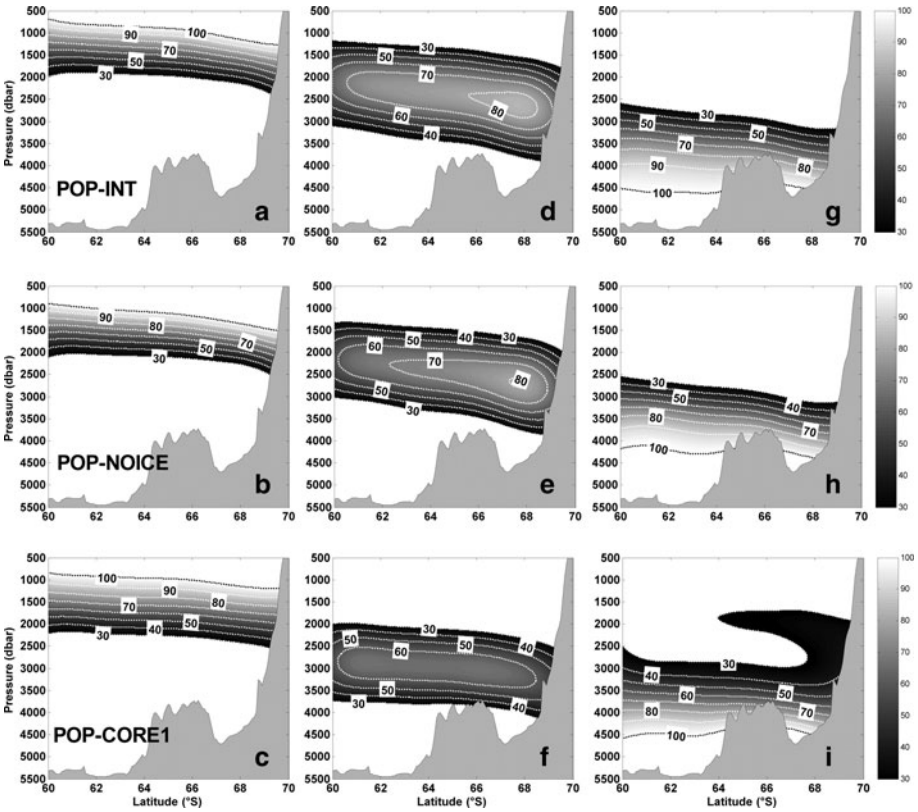

Fig. 8. Dense water mass distribution (% of mixing) at the Greenwich Meridian section obtained from POP-INT, POP-NOICE, and POP-CORE1 simulations, as indicated in the first box, using the water type index based on each model output (see Table II). Each column indicates specifics water masses: **a–c.** Warm Deep Water, **d–f.** Weddell Sea Deep Water, and **g–i.** Weddell Sea Bottom Water. The seamount is the Maud Rise.

mass and the same weight was applied for both θ and salinity. In this approach, the OMP analysis is able to distinguish all the deep water masses at the Greenwich section for all simulations. Based on the results of the previous analysis, the POP-CORE1 simulation represents an improvement because, as discussed earlier, the salinity values are closer to the observations and differ for all water masses used (see Table II). This allowed a refined separation of WSDW and WSBW in deeper layers. Compared to the observed water mass distribution, the representation of all water masses is improved when the interannual forcing is used (POP-INT). Note that this simulation does not incorporate the interactive sea-ice model, but accounts for the intra-seasonal forcing corrected for sea-ice.

Visually, the WDW base limit with a 30% contribution (Fig. 8a–c) fits well with the distribution obtained from observed data (Fig. 5a). However, the WDW contribution to the total mixture varies slightly (∼20–30%) between the simulations and the observational results, as indicated by low RMS differences (∼20%). Although the RMS differences are slightly higher for the POP-NOICE run, they also show a realistic representation for WDW. In the water column, the RMS differences (not shown) show that the layer near the base limit of the WDW (∼1000–2000 m) is better represented than that closer to the surface (∼500–1000 m).

It becomes possible to distinguish deep waters when water mass indices based on the simulation results for all model runs are used (Fig. 8d–f). However, the thickness of the WSDW layer is underestimated compared to observations (Fig. 5b). The upper level of the WSDW layer is not adequately represented, probably because only one water type was used, as described earlier. Nevertheless, the RMS differences show the same behaviour for the WSDW as for the WDW along the section. In this case, the results of the POP-INT and POP-NOICE runs are much closer to the observed pattern (differing ∼15%) than that of the POP-CORE1 run (∼25%). At depth for the POP-INT and POP-NOICE runs, the WSDW layer is better represented between 1500 and 3000 m than the top layer (above 1500 m). This can be seen relative to the distribution with contributions below 30% in this depth interval (Fig. 8d & e). Conversely, for the POP-CORE1 simulation, the WSDW core is displaced downward (Fig. 8f), implying that the depth interval between 1000 and 2000 m is weakly represented (Fig. 8f). Considering the bottom layer, the WSBW is well represented in all simulations at the Greenwich Meridian (Fig. 8g–i) despite the increasing RMS differences (∼20% to 40%) along the entire section and depth. The pattern in RMS differences can be associated with the weak representation of the near-bottom layer properties in the model simulations. Along the latitude regions where the WSBW is expected to fill the water column (i.e. region north of Maud Rise), the RMS differences are constant, around 20%.

The upward shift of the RMS difference curves at high, near-coastal latitudes (between 66°S and 70°S; Fig. 7) is an

https://doi.org/10.1017/S0954102009001825 Published online by Cambridge University Press

indication that near-coastal waters are underrepresented, relative to open ocean waters in the OMP analysis. Considering the bottom layer (WSBW), the missing or incorrect representation of the near-bottom layers suggests that the physical processes that govern the formation and spreading of dense water also requires attention.

It is important to note that the water mass distributions discussed in this section were obtained using different water type indices for each model simulation (Table II). Thus, water mass distributions should not be compared across models. Consequently, the POP-CORE1 water mass distribution cannot be considered the worst simulation to represent the deep water masses. Nevertheless, the previous analyses and the model observation property comparisons clearly show that the inclusion of a sea-ice model in the NCAR-CCSM ocean model leads to a better simulation of the deep ocean.

The work presented here is somewhat sensitive to the choices of water masses and weights, which implies that results may vary depending on the set of OMP parameters used (i.e. water types) and the property weights applied. This demonstrates the challenges inherent not only in correct simulation of water masses in the Southern Ocean but also in evaluation of model results. These models lack the resolution and the representation of some smaller-scale physical processes needed to correctly represent the temperature and salinity range found over the continental shelves of Antarctica. The coarse representation likely also contributes to erroneous representation of several deep ocean characteristics in those models.

Conclusions

This study examines the dense water masses of the Southern Ocean (found in the Weddell Sea) simulated in the NCAR-CCSM model and quantitatively compares them with an observational dataset. We also analyse in detail what would change if an interactive sea-ice model were coupled to the ocean component of the climate model. Results with respect to the impacts of sea-ice simulations in POP-CORE1 are not clear-cut: the OMP results from this simulation are not adequate for all the water masses and for the entire depth interval considered along the section. This reinforces the idea that the representation of ocean-ice processes, and hence dense water formation, is much more complex than having sea-ice alone. A combination of physical processes and refined model resolution may be needed to capture the important interactions that take place within the continental shelf. As highlighted in this text, the sea-ice model helps but does not solve the issue of the strong vertical salinity gradient in the deep layers of the Southern Ocean used to distinguish the different deep water masses. In addition, the recognition of specific water masses in model output is sensitive to the property indices used.

The Southern Ocean is a crucial region of the world because it is the source area of major ocean water masses that are exported to the mid-latitudes and tropics at depth. In addition, this region connects the three major ocean basins and is a major component of the global ocean overturning. Despite this, the Southern Ocean has not been well represented in climate models, and little attention has been paid to the representation of water mass formation and transformation rates. The coupled air-ice-ocean fluxes associated with brine rejection, changing ocean transport and mixing help to improve the simulated dense water mass distributions but more work is clearly required. Despite their known importance to dense water formation in the Southern Ocean, relevant small scale sea-ice processes are normally not accounted for in climate models (Timmermann *et al.* 2002, Beckmann & Goosse 2003, Thoma *et al.* 2006). Better representation of continental shelf and slope processes in high latitude regions, as well as ice shelf fluxes, is needed in order to achieve a better representation of the deep ocean in models. The results presented here emphasize the need to consider interactive cryospheric processes in OGCMs.

Acknowledgments

We thank L. Pezzi, M.E.C. Bernardes, and B.C. Franco for their early suggestions and manuscript improvements. W. Large, P. Gent, M. Raphael, and H.H. Hellmer provided comments that resulted in substantial improvements to this study. Special thanks go to NCAR/OCE for providing the model outputs. This study is a contribution to the GOAL Project supported by grants from the Brazilian Antarctic Program (PROANTAR) and the Council for Research and Scientific Development (CNPq-550370/02-1; 520189/2006-0; 300223/1993-5; 300163/2006-6) of Brazil. We also wish to thank support from grants NSF0327268 and FAPESP-05/03161-9, and two reviewers for their constructive comments, which greatly improved the manuscript. R. Kerr is supported by the CAPES Foundation.

References

Beckmann, A. & Goosse, H. 2003. A parameterization of ice shelf-ocean interaction for climate models. *Ocean Modelling*, **5**, 157–170.

Briegleb, B.P., Bitz, C.M., Hunke, E.C., Lipscomb, W.H., Holland, M.M., Schramm, J.L. & Moritz, R.E. 2004. *Scientific description of the sea-ice component in the Community Climate System Model,* version three. Boulder, CO: National Center for Atmospheric Research, Technical Note NCAT/TN-463 + STR, 70 pp.

Carmack, E.C. 1977. Water characteristics of the Southern Ocean south of the Polar Front. *In* Angel, M.A., *ed. Voyage of Discovery, George Deacon 70th Anniversary volume*. Oxford: Pergamom Press, 15–41.

Carmack, E.C. & Foster, T.D. 1975. On the flow of water out of the Weddell Sea. *Deep-Sea Research*, **22**, 711–724.

Connolley, W.M. & Bracegirdle, T.J. 2007. An Antarctic assessment of IPCC AR4 coupled models. *Geophysical Research Letters*, **34**, 10.1029/2007GL031648.

Danabasoglu, G. 2004. A comparison of global ocean general circulation model solutions with synchronous and accelerated integration methods. *Ocean Modelling*, **7**, 323–341.

Deacon, G.E.R. 1979. The Weddell Gyre. *Deep-Sea Research*, **26A**, 981–995.

Doney, S.C. & Hecht, M.W. 2002. Antarctic bottom water formation and deep-water chlorofluorocarbon distributions in a global ocean climate model. *Journal of Physical Oceanography*, **32**, 1642–1666.

Fahrbach, E., Rohardt, G., Schröder, M. & Strass, V. 1994. Transport and structure of the Weddell Gyre. *Annales Geophysicae*, **12**, 840–855.

Fahrbach, E., Harms, S., Rohardt, G., Schröder, M. & Woodgate, R.A. 2001. Flow of bottom water in the northwestern Weddell Sea. *Journal of Geophysical Research*, **106**, 2761–2778.

Fahrbach, E., Hoppema, M., Rohardt, G., Schröder, M. & Wisotzki, A. 2004. Decadal-scale variations of water mass properties in the deep Weddell Sea. *Ocean Dynamics*, **54**, 77–91.

Fahrbach, E., Rohardt, G., Scheele, N., Schröder, M., Strass, V. & Wisotzki, A. 1995. Formation and discharge of deep and bottom water in the northwestern Weddell Sea. *Journal of Marine Research*, **53**, 515–538.

Fichefet, T. & Maqueda, M.A.M. 1997. Sensitivity of a global sea-ice model to the treatment of ice thermodynamics and dynamics. *Journal of Geophysical Research*, **102**, 12 609–12 643.

Foldvick, A., Gammelsrod, T. & Torreson, T. 1985. Circulation and water masses on the southern Weddell Sea shelf. *Antarctic Research Series*, **43**, 5–20.

Foster, T.D. & Carmack, E.C. 1976. Frontal zone mixing and Antarctic bottom water formation in the southern Weddell Sea. *Deep-Sea Research*, **23**, 301–317.

Foster, T.D. & Carmack, E.C. 1977. Antarctic bottom water formation in the Weddell Sea. *In* Dunbar, M.J., *ed. Polar oceans*. Montreal: Arctic Institute of North America, 167–177.

Gent, P.R., Bryan, F., Danabasoglu, G., Doney, S., Holland, W., Large, W. & McWilliams, J.C. 1998. The NCAR Climate System Model global ocean component. *Journal of Climate*, **11**, 1287–1306.

Gordon, A.L. 1998. Western Weddell Sea thermohaline stratification. *Antarctic Research Series*, **75**, 215–240.

Gordon, A.L & Huber, B.A. 1984. Thermohaline stratification below the southern ocean sea-ice. *Journal of Geophysical Research*, **89**, 641–648.

Gordon, A.L., Visbeck, M. & Huber, B. 2001. Export of Weddell Sea deep and bottom water. *Journal of Geophysical Research*, **106**, 9005–9017.

Gouretski, V.V. & Danilov, A.I. 1993. Weddell Gyre: structure of the eastern boundary. *Deep-Sea Research I*, **40**, 561–582.

Griffies, S., Biastoch, A., Boning, C., Bryan, F., Danabasoglu, G., Chassignet, E.P., England, M., Gerdes, R., Haak, H., Hallberg, R.W., Hazeleger, W., Jungclaus, J., Large, W.G., Madec, G., Pirani, A., Samuels, B.L., Scheinert, M., Sen Gupta, A., Severijns, C.A., Simmons, H.L., Treguier, A.M., Winton, M., Yeager, S. & Yin, J. 2009. Coordinated Ocean-ice reference Experiments (COREs). *Ocean Modelling*, **26**, 1–46.

Holland, M.M., Bitz, C.M., Hunke, E.C., Lipscomb, W.H. & Schramm, J.R. 2006. Influence of the ice thickness distribution on Polar Climate in CCSM3. *Journal of Climate*, **19**, 2398–2414.

Huntley, H.S., Tabak, E.G. & Suh, E.H. 2007. An optimization approach to modeling sea-ice dynamics. Part 1: Lagrangian framework. *Journal of Applied Mathematics*, **67**, 543–560.

Karstensen, J. & Tomczak, M. 1997. Ventilation processes and water mass ages in the thermocline of the southeast Indian Ocean. *Geophysical Research Letters*, **24**, 2777–2780.

Karstensen, J. & Tomczak, M. 1998. Age determination of mixing water masses using CFC and oxygen data. *Journal of Geophysical Research*, **103**, 18 599–18 609.

Kerr, R. 2006. *Distribuição, Mistura e Variabilidade das massas de água profundas do Mar de Weddell, Antártica.* MSc thesis, Fundação Universidade Federal do Rio Grande (FURG), 146 pp. Available at www.oceanfisquigeo.furg.br/producao

Kerr, R., Mata, M.M. & Garcia, C.A.E. 2005. Optimum multiparameter analysis of the Weddell Sea water mass structure. *Clivar Exchanges*, **10**(4), 33–35.

Klatt, O., Fahrbach, E., Hoppema, M. & Rohardt, G. 2005. The transport of the Weddell Gyre across the Prime Meridian. *Deep-Sea Research II*, **52**, 513–528.

Large, W.G., McWilliams, J.C. & Doney, S.C. 1994. Oceanic vertical mixing: a review and a model with a non-local boundary layer parameterization. *Reviews of Geophysics*, **32**, 363–403.

Large, W.G., Danabasoglu, G., Doney, S.C. & McWilliams, J.C. 1997. Sensitivity to surface forcing and boundary layer mixing in a global ocean model: annual-mean climatology. *Journal of Physical Oceanography*, **27**, 2418–2447.

Large, W. & Yeager, S. 2004. *Diurnal to decadal global forcing for ocean and sea-ice models: the datasets and flux climatology*. Boulder, CO: CGD Division, National Center for Atmospheric Research, NCAR/TN-460 + STR.

Large, W.G. & Danabasoglu, G. 2006. Attribution and impacts of upper ocean biases in CCSM3. *Journal of Climate*, **19**, 2325–2346.

Leffanue, H. & Tomczak, M. 2004. Using OMP analysis to observe temporal variability in water mass distribution. *Journal of Marine Research*, **48**, 3–14.

Lipscomb, W.H. & Hunke, E.C. 2004. Modeling sea-ice transport using incremental remapping. *Monthly Weather Review*, **132**, 1341–1354.

Mackas, D.L., Denman, K.L. & Bennett, A.F. 1987. Least squares multiple tracer analysis of water mass composition. *Journal of Geophysical Research*, **92**, 2907–2918.

Mamayev, O.I. 1975. *Temperature-salinity analysis of world ocean waters*. Amsterdam: Elsevier, 374 pp.

OMP2. 2005. *Water mass analysis package*. Available at http://www.ldeo.columbia.edu/~jkarsten/omp_std/

Orsi, A.H., Nowlin, W.D. & Whitworth, T. 1993. On the circulation and stratification of the Weddell Gyre. *Deep-Sea Research I*, **40**, 169–303.

Orsi, A.H., Johnson, G.C. & Bullister, J.L. 1999. Circulation, mixing, and production of Antarctic bottom water. *Progress in Oceanography*, **43**, 55–109.

Orsi, A.H., Whitworth, T. & Nowlin, W.D. 1995. On the meridional extent and fronts of the Antarctic Circumpolar Current. *Deep-Sea Research I*, **42**, 641–673.

Robertson, R., Visbeck, M., Gordon, A.L. & Fahrbach, E. 2002. Long-term temperature trends in the deep waters of the Weddell Sea. *Deep-Sea Research II*, **49**, 4791–4806.

Smith, R.D. & Gent, P. 2004. *Reference manual for the Parallel Ocean Program* (*POP*)*, ocean component of the Community Climate System Model* (*CCSM2.0*). Los Alamos, NM: Los Alamos National Laboratory, Technical Report LAUR-02-2484.

Smith, R.D. & McWilliams, J.C. 2003. Anisotropic horizontal viscosity for ocean models. *Ocean Modelling*, **5**, 129–156.

Thoma, M., Grosfeld, K. & Lange, M.A. 2006. Impact of the eastern Weddell ice shelves on water masses in the eastern Weddell Sea. *Journal of Geophysical Research*, **111**, 10.1029/2005JC003212.

Timmermann, R., Hellmer, H.H. & Beckmann, A. 2002. Simulations of ice-ocean dynamics in the Weddell Sea. 2. Interannual variability 1985–1993. *Journal of Geophysical Research*, **107**, 10.1029/2000JC000742.

Tomczak, M. 1981. A multi-parameter extension of temperature/salinity diagram techniques for the analysis of non-isopycnal mixing. *Progress in Oceanography*, **10**, 147–171.

Tomczak, M. 1999. Some historical, theoretical and applied aspects of quantitative water mass analysis. *Journal of Marine Research*, **57**, 275–303.

Tomczak, M. & Large, D.G.B. 1989. Optimum multiparameter analysis of mixing in the thermocline of the eastern Indian Ocean. *Journal of Geophysical Research*, **94**, 16 141–16 149.

Tomczak, M. & Godfrey, J.S. 1994. *Regional oceanography: an introduction*. Oxford: Pergamon, 377 pp.

Weppernig, R., Schlosser, P., Khatiwala, S. & Fairbanks, R.G. 1996. Isotope data from Ice Station Weddell: implications for deep water formation in the Weddell Sea. *Journal of Geophysical Research*, **101**, 25 723–25 739.

Yeager, S.G. & Large, W.G. 2007. Observational evidence of winter spice injection. *Journal of Physical Oceanography*, **37**, 2895–2919.